World Journal of Advanced Engineering Technology and Sciences
eISSN: 2582-8266
Cross Ref DOI: 10.30574/wjaets
Journal homepage: https://wjaets.com/

(RESEARCH ARTICLE)

Check for updates

Evaluation of the mechanical properties of orthopedic screw made from bovine cortical bones

Ipilakyaa Tertsegha Daniel *, Atanda Moses and Tuleun Livinus Tyovenda

Department of Mechanical Engineering, Joseph Sarwuan Tarka University, Makurdi, Benue State-Nigeria.

World Journal of Advanced Engineering Technology and Sciences, 2025, 15(02), 612-621

Publication history: Received on 23 March 2025; revised on 29 April 2025; accepted on 01 May 2025

Article DOI: https://doi.org/10.30574/wjaets.2025.15.2.0549

Abstract

Allogeneic cortical bone screws offer a promising alternative to traditional metallic orthopedic screws, primarily due to their potential for improved biocompatibility and osteointegration. However, earlier designs of these biological implants faced significant challenges, including antigenicity, inconsistent mechanical properties, limited bioactivity, and inadequate fixation performance—factors that restricted their clinical adoption. This study addresses these issues through two key innovations: a redesigned screw shape and an optimized processing method for the allogeneic cortical bone material. The new fabrication process involves decellularization of cortical bone to eliminate antigenic components while preserving its mechanical strength. A novel screw geometry was developed to increase surface area and enhance bone-implant interaction. The redesigned shape was aimed at optimizing stress distribution and promoting superior osteointegration. To evaluate the mechanical performance, Stress Transfer Parameters (STP) were measured for both conventional and redesigned screws. For the first thread (α), the STP of redesigned bovine, titanium, and stainless-steel screws were 0.361, 0.145, and 0.136 respectively, compared to 0.116, 0.110, and 0.013 for their conventional counterparts. For the remaining engaged threads (β), the redesigned screws recorded STP values of 0.658, 0.546, and 0.510, significantly outperforming the conventional designs, which had values of 0.128, 0.039, and 0.029 respectively. The results confirm that the redesigned allogeneic cortical bone screws exhibit superior mechanical stability and improved osteointegration. This advancement in both material processing and screw design represents a significant step toward more effective, reliable, and biocompatible orthopedic implants.

Keywords: Bovine Bones; Orthopedic Screws; Allogeneic Cortical Bones; Stress Transfer Parameters; Osteointegration

1. Introduction

Orthopedic implants, such as screws and Plates, play a crucial role in the stabilization and healing of fractured bones. Traditionally, these devices have been manufactured using metallic materials like stainless steel and titanium alloys due to their high mechanical strength and corrosion resistance. However, these materials often present challenges such as stress shielding, corrosion-related complications, high production costs, and difficulties with biodegradability, which can hinder long-term integration with the host tissue (Meng et al., 2023; Al-Shalawi et al., 2023).

In recent years, the exploration of biocompatible and biodegradable materials for orthopedic applications has gained traction. Among the alternatives, natural biomaterials derived from animal sources, particularly bovine bones, have shown promise due to their inherent biocompatibility, structural similarity to human bone, and cost-effectiveness. Bovine cortical bone, in particular, possesses favorable mechanical properties that suggest its potential use as a raw material for orthopedic screw fabrication (Li et al., 2025).

* Corresponding author: Ipilakyaa Tertsegha Daniel.

Despite the promise of bovine bone-derived implants, limited studies have thoroughly investigated the mechanical behavior of orthopedic screws made from this material. Furthermore, advancements in computational modeling and finite element simulation provide a powerful platform to predict the mechanical performance of such bio-based implants under physiological loading conditions, thus aiding in the optimization of their design and functionality (Nasr et al., 2022; Su et al., 2022; Sun et al., 2022).

This study seeks to evaluate the mechanical properties and performance of orthopedic screws fabricated from bovine cortical bones through both experimental testing and simulation. By comparing the results to conventional materials, the research aims to assess the feasibility of adopting bovine-derived orthopedic implants in clinical practice, potentially paving the way for more sustainable and biologically compatible orthopedic solutions.

2. Methods

Bovine bone sample (Cattle tibiae) was harvested from the medial-diaphyseal portion of bovine tibia at a local abattoir in Gwagwalada FCT Abuja Nigeria. Cortical bone from bovine tibia was collected and de-fleshed, as shown in Figure 1. The was dissected in fragments of rods of approximate diameter of 15-20mm using a cleaver (Figure 2). The samples were then machined into dog bone shape according to DIN EN ISO 527-2 using a CNC (Computer Numerical Control) lathe machine. Finally, the samples were milled to flat samples of 2mm thickness base on the dimensions. Some key mechanical property tests were performed on the decellularized sample material using universal testing machine TIRAtest 2810 & Eltex Tera-ohm- meter 6206.

Figure 1 De-fleshing of bovine femur

Figure 2 Bone shaped in rod-like form

3. Design

The design of rectangular thread cancellous screw made of bovine cortical bone equivalent to a 6.5mm conventional metallic cancellous screw was considered for two failure criteria: failure of the screw through screw core sharing and failure through screw thread striping (Feng et al., 2022).

From the first failure criterion and the value of the compressive strength Table 1 of the bovine cortical bone sample the minimum core diameter 'd_0' of the screw was determined as

$$d_0 = 5.16mm$$

Going by the Stress Transfer Parameters STPs

For the first engaged thread.

$$\alpha = \frac{\sigma_{fb}}{\sigma_{ft}} \qquad \text{..... (1a)}$$

for the subsequent engaged threads.

$$\beta = \left[\frac{1}{N}\sum_{i=2}^{N}\sigma_{b_i} \Big/ \frac{1}{N}\sum_{J}^{N}\sigma_{t_j}\right] \qquad \text{.....(1b)}$$

Where σ = stress,

- f = first, b = bone thread, t = screw thread,
- N = total number of engaged threads.
- i,j = particular thread under consideration

We seek the value of thread ratio $\frac{y_1}{y_2}$ Figure 3 that made the shear stress at the root of a pair of the engaged thread equal and consequently $\alpha \cong 1$, and $\beta \cong 1$

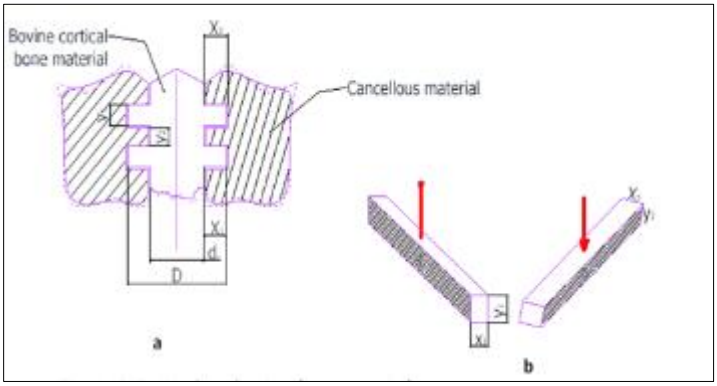

Figure 3 Section at engagement point of thread on the screw and the thread in the femur head

Consideration of the second failure criterion of the screw give rise to

$$\frac{\tau_{u2}}{\tau_{u1}} = \frac{A'_1}{A'_2} = \frac{y_1 \pi d}{y_2 \pi D} = 0.593 \quad \ldots\ldots (2)$$

$$y_1 = \frac{0.593D}{d_o} y_2 \quad (3)$$

When $d = 5.1$mm and D = 7.6mm

$$y_1 = 0.884 y_2 \quad (4)$$

4. Results

Results for mechanical properties of the produced bovine bones are presented below.

Table 1 Results for Mechanical Properties of Bovine Bones

S/No	Test	Value Mpa	Reported Range (Mpa)	Standard	Test Machine
1	Tensile Strength	135	80 -150	ASTM D 3039	TRAtest 2810
2	Compressive Strength	152	130 -180	ASTM D 6641	TRAtest 2810
3	Flexural Strength	90		ASTM D 790	TRAtest 2810
4	Shear Strength	52	50-130	ASTM D379	Tonny Press11

Simulation results for the equivalent (Von – Mises) stress at probed points for the designed and conventional profile screw thread for the bovine compared with the metallic screws shown in Figures 4 and 5

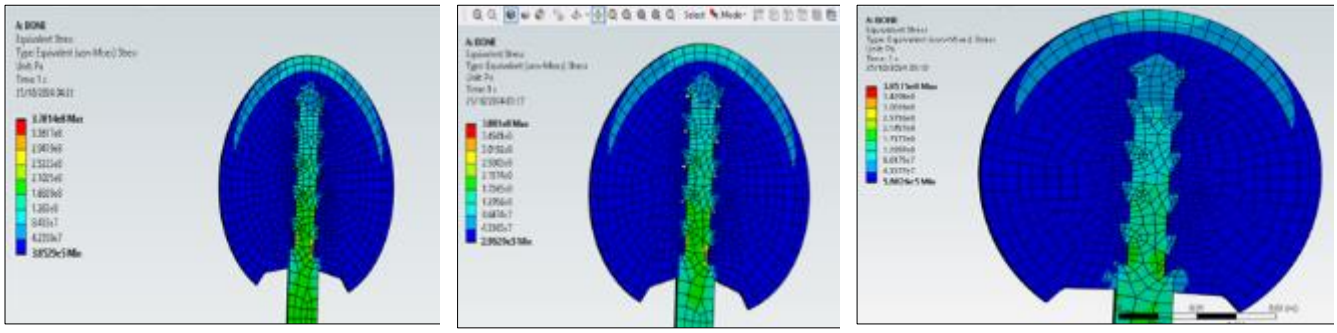

A Bovine screw material **B Titanium screw material** **C Stainless steel screw material**

Figure 4 Von-mises Stress for designed screw

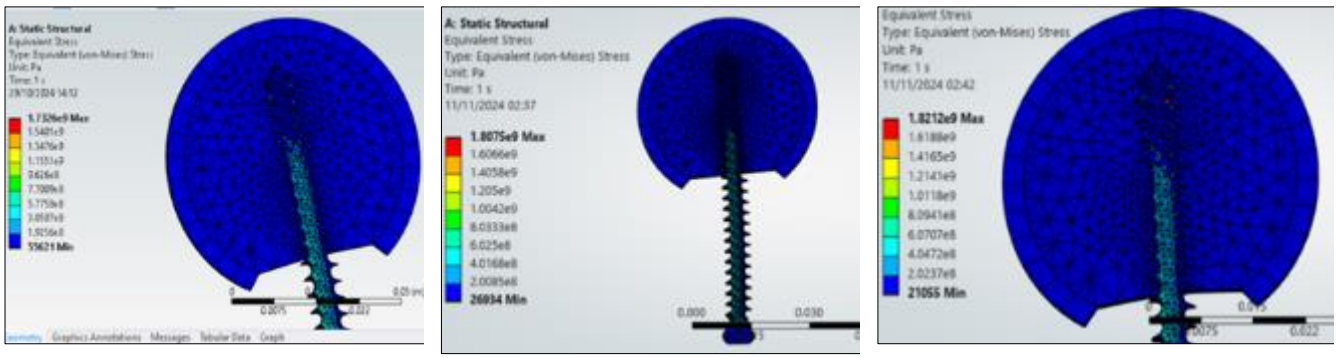

A Stress for bovine screw **B Stress for Ti6Al4V screw** **C Stress for 316L**

Figure 5 Von-mises stress for standard 6.5mm cancellous screw

Table 2 Stress values at probed points when redesigned screw material is bovine cortical material

S/No	Thread on Femur Head		Thread on Screw		STP
	node id	stress $\sigma_f$value (x107) pa	node id	stress $\sigma_s$value (x107) pa	
1	2054	3.618	2383	5.647	0.641
2	2042	3.568	2371	6.082	0.587
3	2021	4.201	2359	7.128	0.589
4	1997	5.412	2347	8.825	0.613
5	1975	9.339	2541	12.009	0.6.95
6	2081	6.359	2529	26.507	0.361

Table 3 Stress values at points when the redesigned screw material is TitaniumTi6Al4V

S/NO	Thread On Femur Head		Thread On Screw		STP
	Node Id	Stress σ_f Value(X10^7) Pa	Node Id	Stress σ_{Ti} Value(X10^7) Pa	
1	2054	4.814	2383	6.852	0.703
2	2042	5.039	2371	7.441	0.677
3	2021	5.282	2359	8.884	0.594
4	1997	6.169	2347	11.574	0.533
5	1975	6.147	2541	15.498	0.397
6	2081	4.830	2529	33.300	0.136

Table 4 Stress values at probed points when redesigned screw material is stailess steel 316L

S/No	Thread in Femur Head		Thread On Screw		STP
	Node Id	Stress σ_fValue(X10^7) Pa	Node Id	Stress σ_sValue(X10^7) Pa	
1	2054	4.891 `````	2383	7.195	0.680
2	2042	5.127	2371	7.527	0.681
3	2021	5.347	2359	9.060	0.590
4	1997	6.210	2347	11.820	0.525
5	1975	4.128	2541	15.794	0.261
6	2081	4.696	2529	34.635	0.136

Table 5 Stress values at points when conventional screw material is bovine cortical bone.

S/No	Thread On Screw		Thread On Femur Head		STP
	Node Id	Stress σ_s Value(X10^7) Pa	Node Id	Stress σ_fValue(X10^7) Pa	
1	572	6.181	12473	1.230	0.198
2	3920	1.127	12493	0.267	0.237
3	3870	1.215	1221	0.245	0.202
4	3823	1.022	12249	0.218	0.213
5	1242	1.396	12277	0.225	0.161
6	1238	1.789	12305	0.139	0.077
7	3679	3.665	12333	0.261	0.071
8	7245	5.524	12361	0.268	0.048
9	7229	4.062	12359	0.395	0.097
10	7215	7.621	12417	1.048	0.136
11	7542	14.562	12441	2.166	0.149

Table 6 Stress values at probed points when conventional screw material is Titanium Ti6Al4V

S/No	Thread On Femur Head		Thread On Screw		STP
	Node Id	Stress σ_fValue (X10^7) Pa	Node Id	Stress σ_sValue (X10^7) Pa	
1	572	8.759	12493	2.456	0.280
2	3920	25.049	12493	0.3964	0.016
3	3870	9.289	1221	0.3400	0.042
4	3823	15.068	12249	0.3157	0.021
5	1242	16.033	12277	0.2628	0.016
6	1238	15.062	12305	0.2323	0.015
7	3679	16.945	12333	0.1512	0.009
8	7245	14.253	12361	0.3247	0.023
9	7229	13.894	12359	0.595	0.043
10	7215	13.763	12417	0.7464	0.054
11	7542	17.088	12441	1.9851	0.116

Table 7 Stress values at probed points when convetional screw material is stainless steel 316L

S/No I	Thread On Screw		Thread On Femur Head		STP
	Node Id	Stress σ_sValue (X10^7) Pa	Node Id	Stress σ_fValue (X10^7) Pa	
1	572	1.829	12473	1.797	0.983
2	3920	6.541	12493	1.292	0.198
3	3870	39.001	1221	1.153	0.029
4	3823	33.806	12249	0.392	0.012
5	1242	32.325	12277	0.365	0.011
6	1238	29.807	12305	0.362	0.012
7	3679	34.226	12333	0.310	0.009
8	7245	32.816	12361	0.428	0.013
9	7229	27.838	12359	0.603	0.022
10	7215	19.491	12417	0.870	0.045
11	7542	13.429	12441	0.180	0.013

Results for analysis on stress transfer parameters is compared in Figures 6 and 7 for the redesigned screw with the conventional screw when the material is bovine cortical bone, titanium and stainless steel.

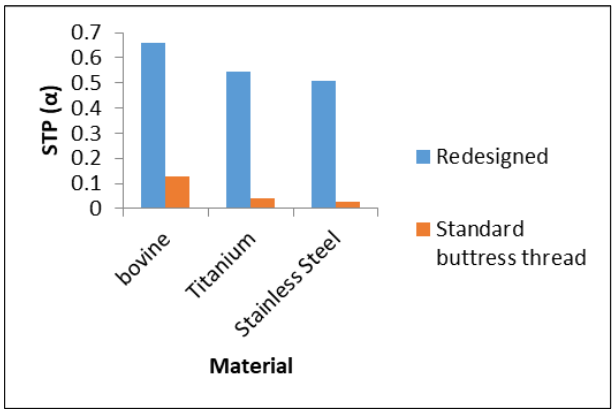

Figure 6 Simulated STP value for α of redesigned screw compared with standard buttress thread screw

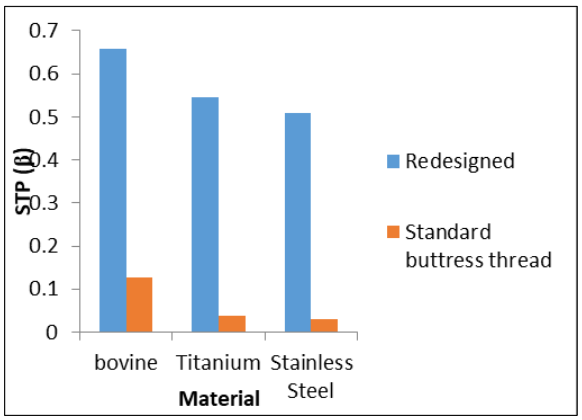

Figure 7 Simulated STP value for β of redesigned screw compared with standard buttress thread screw

5. Discussions

The mechanical properties of the bovine bone screw and associated assembly materials were defined based on mechanical test results and integrated into the simulation solver. All materials were treated as isotropic and continuous. The properties assigned to the cortical bovine bone screw align with previous findings, such as those by Elahi et al., (2025), who reported a Young's modulus of approximately 18 GPa and a Poisson's ratio of 0.3. The tensile strength and fatigue resistance values exceed those of cancellous bone, reflecting the denser and stiffer nature of cortical bone. Literature, including Metzner et al., (2021), supports the use of bovine bone in orthopedic implants, especially when treated or coated to improve fatigue resistance.

Cancellous bone exhibits significantly lower mechanical properties. For instance, Zhang et al., (2022) reported a Young's modulus between 0.1 and 0.4 GPa, with our model adopting values between 0.1 and 0.3 GPa. Its lower density and porous structure limit its load-bearing capacity. Despite this, a consistent Poisson's ratio of 0.3 is used across studies, including Ma et al., (2023).

When compared to conventional implant materials, the differences are stark. Titanium (Ti-6Al-4V) has a Young's modulus of ~110 GPa, while stainless steel (AISI 316L) reaches ~200 GPa. These materials, though strong, present a stiffness mismatch with bone, potentially leading to stress shielding and bone resorption (Li et al., 2025). The bovine bone screw, with more bone-like mechanical properties, offers potential for better biocompatibility and osteointegration.

5.1. 3D Modeling and Simulation

ANSYS SpaceClaim was used to design the screw and model the human femur bone based on CT scan data converted from STL to solid geometry. Figure 8 illustrates the 3D models and meshed assembly. A 48 mm section from the femoral head simulated a typical fracture site, relevant for orthopedic screw fixation (Boháč et al., 2025).

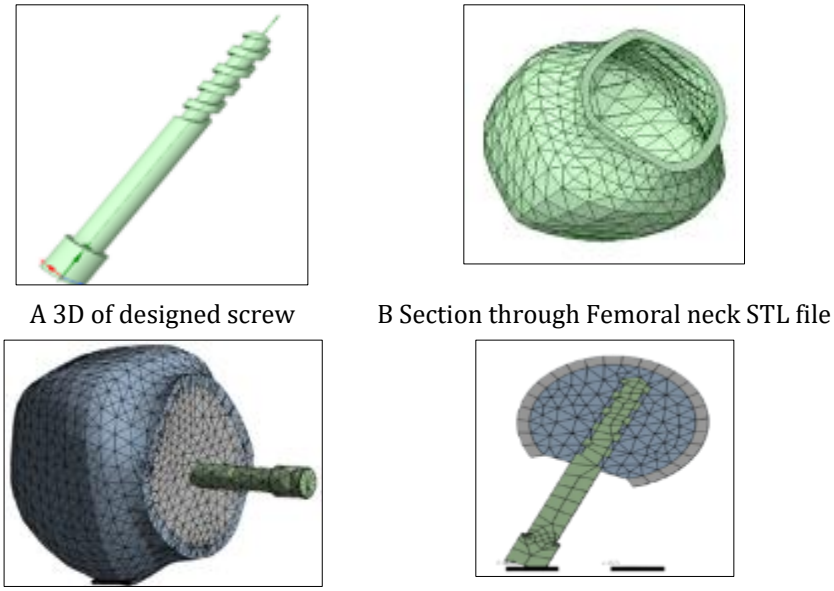

A 3D of designed screw B Section through Femoral neck STL file

C 3D assembly of installed screw D Meshed simplified model

Figure 8 3D modeling

The assembly model, meshed with 703 tetrahedral elements and 2460 nodes, employed shared topology to ensure interface accuracy between cortical and cancellous bone. Stress analysis focused on thread-bone interaction under load, a crucial factor in insertion torque and fatigue performance (Deng et al., 2023). Material properties were assigned based on literature values to ensure realistic simulation outputs.

Model simplification, mesh optimization, and adaptive meshing in high-stress regions improved computational efficiency while maintaining accuracy (Shakour & Amir, 2022). The analysis was structured into seven subsections to systematically evaluate screw performance.

5.2. Stress and Deformation Analysis

Simulation results indicate that the rectangular thread profile produced the highest STP (0.658), outperforming the standard buttress thread (0.128), confirming earlier findings by Narayankar et al., 2022). Titanium screws (STP 0.546) transferred stress more efficiently than stainless steel (STP 0.510), though stress distribution (α vs. β) showed minimal variation, contrary to Gefen's assumption of a dominant first thread stress.

Higher STP values correlated with greater deformation, especially in the bovine screw, indicating increased stress transfer to surrounding bone. This supports findings by Jia et al., (2025) and Wang et al., (2023). Stress-time plots showed stress shielding in the early loading stages, with buttress threads causing higher stress concentrations over time due to larger bone contact areas.

Notably, bovine bone became brittle after five days of preparation, complicating machining and possibly affecting simulation accuracy. While all materials were modeled as isotropic due to software limitations, bone is inherently anisotropic—a factor that future studies should consider for more realistic modeling (Zhang et al., 2023)

5.3. Stress Transfer Comparison Across Materials

Stress Transfer Parameters (STP) for different materials and thread designs revealed that:

- **Bovine Cortical Bone** (STP = 0.145, rectangular): Exhibits the highest efficiency in stress transfer due to bone-like stiffness.

- **Titanium Ti6Al4V** (STP = 0.136, rectangular): Offers a good balance of biocompatibility and stress transfer.
- **Stainless Steel 316L** (STP = 0.546, rectangular): High stiffness leads to stress shielding.

In buttress thread designs:

- STP dropped across all materials, with Titanium showing the lowest (0.013) and Bovine bone dropping to 0.11, reaffirming the rectangular thread's superiority in biomechanical performance.

These results confirm that both thread geometry and material stiffness critically influence implant performance. Rectangular threads enhance stress transfer, while bovine cortical bone presents a promising alternative to conventional metals due to its biomechanical compatibility.

6. Conclusion

The study successfully designed and analyzed a bovine cortical bone screw for femoral head fracture fixation. Compared to conventional materials, bovine bone exhibited better mechanical compatibility based on stress transfer metrics. The analysis supports the use of rectangular threads for improved load distribution and highlights the potential of bovine bone as a viable implant material. Future studies should incorporate anisotropic modeling and fatigue analysis to further validate these findings.

Compliance with ethical standards

Disclosure of conflict of interest

No conflict of interest to be disclosed.

References

[1] Al-Shalawi, F. D., Ariff, A. H. M., Jung, D., Ariffin, M. K. a. M., Kim, C. L. S., Brabazon, D., & Al-Osaimi, M. O. (2023). Biomaterials as Implants in the Orthopedic Field for Regenerative Medicine: Metal versus Synthetic Polymers. Polymers, 15(12), 2601. https://doi.org/10.3390/polym15122601

[2] Azadani, M. N., Zahedi, A., Bowoto, O. K., & Oladapo, B. I. (2022). A review of current challenges and prospects of magnesium and its alloy for bone implant applications. Progress in Biomaterials, 11(1), 1–26. https://doi.org/10.1007/s40204-022-00182-x

[3] Boháč, P., Apostolopoulos, V., Marcián, P., Tomáš, T., Mahdal, M., & Návrat, T. (2025). Computational modeling of bone allograft reconstruction following femoral shaft tumor resection: Investigating the impact of supplementary plate fixation. PLoS ONE, 20(2), e0316719. https://doi.org/10.1371/journal.pone.0316719

[4] Deng, Z., Jiang, J., Chen, Z., Zhang, W., Yao, Q., Song, C., Sun, Y., Yang, Z., Yan, S., Huang, Q., & Bajaj, C. (2023). TAssembly: Data-driven fractured object assembly using a linear template model. Computers & Graphics, 113, 102–112. https://doi.org/10.1016/j.cag.2023.05.003

[5] Elahi, A., Duncan, W., Li, K. C., Bhattacharjee, T., & Coates, D. (2025). Supercritical CO2 with enzymatic posttreatment enhances mechanical and biological properties of cancellous bovine bone block grafts. Journal of Biomedical Materials Research Part A, 113(3). https://doi.org/10.1002/jbm.a.37896

[6] Feng, X., Zhang, S., Luo, Z., Liang, H., Chen, B., & Leung, F. (2022). Development and initial validation of a novel thread design for nonlocking cancellous screws. Journal of Orthopaedic Research®, 40(12), 2813–2821. https://doi.org/10.1002/jor.25305

[7] Jia, X., Xie, Y., Yang, Y., Deng, Y., Zhang, K., Shen, C., Li, Y., & Ma, L. (2025). Comparative analysis of three vertebral screw placement directions in anterior thoracolumbar Fracture Surgery: A Finite element study. Orthopaedic Surgery. https://doi.org/10.1111/os.70017

[8] Li, J., Li, Q., Deng, Y., Zhang, W., & Yin, H. (2025). Micro-Abrasive air jet machining technology for fabrication of helical grooves on bovine bone. Micromachines, 16(2), 149. https://doi.org/10.3390/mi16020149

[9] Li, S., Chen, B., Hao, S., Yeom, J., Nam, T., & Wang, X. (2025). Low modulus and high strength in a β Ti alloy exhibiting near-linear deformation behavior and TRIP/TWIP effect for potential biomedical applications. Journal of Alloys and Compounds, 179448. https://doi.org/10.1016/j.jallcom.2025.179448

[10] Ma, Y., Zhao, F., Liu, J., Zhang, Y., Xu, Y., Zhang, P., Gao, S., & Zhang, J. (2023). Dynamic mechanical properties, interface structure evolution and deformation behaviors of PVA-carbon fiber reinforced concrete with negative Poisson's ratio design. Construction and Building Materials, 391, 131897. https://doi.org/10.1016/j.conbuildmat.2023.131897

[11] Meng, M., Wang, J., Huang, H., Liu, X., Zhang, J., & Li, Z. (2023). 3D printing metal implants in orthopedic surgery: Methods, applications and future prospects. Journal of Orthopaedic Translation, 42, 94–112. https://doi.org/10.1016/j.jot.2023.08.004

[12] Metzner, F., Neupetsch, C., Fischer, J., Drossel, W., Heyde, C., & Schleifenbaum, S. (2021). Influence of osteoporosis on the compressive properties of femoral cancellous bone and its dependence on various density parameters. Scientific Reports, 11(1). https://doi.org/10.1038/s41598-021-92685-z

[13] Narayankar, A., Aswal, G. S., Ahmed, S., Kumar, V., Rawat, R., & Prabhakar, N. (2022). Stress distribution patterns associated with dental implants with varying thread designs, dimensions, and splinting conditions: A photoelastic analysis. World Journal of Dentistry, 13(1), 9–15. https://doi.org/10.5005/jp-journals-10015-1885

[14] Shakour, E., & Amir, O. (2022). Stress-constrained topology optimization with precise and explicit geometric boundaries. Structural and Multidisciplinary Optimization, 65(2). https://doi.org/10.1007/s00158-021-03115-7

[15] Su, P., Wang, S., Lai, Y., Zhang, Q., & Zhang, L. (2022). Screw Analysis, Modeling and Experiment on the Mechanics of Tibia Orthopedic with the Ilizarov External Fixator. Micromachines, 13(6), 932. https://doi.org/10.3390/mi13060932

[16] Sun, C., Dong, E., Chen, J., Zheng, J., Kang, J., Jin, Z., Liu, C., Wang, L., & Li, D. (2022). The promotion of mechanical properties by bone ingrowth in Additive-Manufactured Titanium Scaffolds. Journal of Functional Biomaterials, 13(3), 127. https://doi.org/10.3390/jfb13030127

[17] Wang, J., Zhou, Y., Qiao, Z., Goel, S., Wang, J., Wang, X., Chen, H., Yuan, J., & Lyu, B. (2023). Surface polishing and modification of Ti-6Al-4V alloy by shear thickening polishing. Surface and Coatings Technology, 468, 129771. https://doi.org/10.1016/j.surfcoat.2023.129771

[18] Zhang, H., Qi, L., Wang, X., Guo, Y., Liu, J., Xu, Y., Liu, C., Zhang, C., & Richel, A. (2022). Preparation of a cattle bone collagen peptide–calcium chelate by the ultrasound method and its structural characterization, stability analysis, and bioactivity on MC3T3-E1 cells. Food & Function, 14(2), 978–989. https://doi.org/10.1039/d2fo02146c

[19] Zhang, Y., Zhang, Q., He, F., Zuo, F., & Shi, X. (2022). Fabrication of cancellous-bone-mimicking β-tricalcium phosphate bioceramic scaffolds with tunable architecture and mechanical strength by stereolithography 3D printing. Journal of the European Ceramic Society, 42(14), 6713–6720. https://doi.org/10.1016/j.jeurceramsoc.2022.07.033